



## Exergy evaluation of packed bed solar air heater

Mukesh Kumar Lalji<sup>a,\*</sup>, R.M. Sarviya<sup>b</sup>, J.L. Bhagoria<sup>b</sup>

<sup>a</sup> Sardar Vallabh Bhai Polytechnic College, M.P. Govt., Bhopal 462002 (M.P.), India

<sup>b</sup> Department of Mechanical Engineering, MANIT, Govt. of India, Bhopal 462002 (M.P.), India

### ARTICLE INFO

#### Article history:

Received 2 June 2011

Received in revised form

9 April 2012

Accepted 18 April 2012

Available online 30 August 2012

#### Keywords:

Solar air heater

Heat transfer

Wire screen matrices

### ABSTRACT

In view of above present investigation is planned with the following.

The present investigation has been carried out with the following objectives:

- (1) To study performance of packed bed solar air heater for high porosity range and for different shapes of matrices.
- (2) Development of correlations for heat transfer coefficient and friction factor for packed bed solar air heater and its comparison with conventional design.
- (3) Exergy analysis of packed bed solar air heater.

The present study involved outdoor experimental work for generation of heat transfer and friction data for flow in a packed bed solar air heater at different mass flow rates of air for various porosities and shapes of matrices. Data is also collected for conventional smooth duct under similar operating conditions for ensuring accuracy of experimental data. Six matrices had been tested for seven values of flow rates corresponding to flow Reynolds number of about 1000–4700 and data is collected under steady state condition. Ranges of parameters covered in this experimental investigation are as follows:

Reynolds number,  $Re = 1000\text{--}4700$

Porosity,  $P = 0.9614\text{--}0.9984$

Number of layers,  $n = 3\text{--}6$

It is found that in the entire range of Reynolds number, Colburn factor decreases with an increase of packing Reynolds number and volumetric heat transfer increased monotonically with a decrease in porosity. Also from the various matrices studied hexagonal shaped matrix performed lowest of all other matrices. Square shaped matrix performed best amongst the matrices studied.

Following correlations have been developed for Colburn factor and friction factor in terms of porosity and operating parameters:

$$J_h = 0.1765 \left[ (1/nP)^{0.6156} \right] (p_t/d_w)^{0.1229} \left[ 0.6651 Re_p^{-0.4767} \right]$$

$$f_p = 2.0291 \left[ (1/nP)^{0.3521} \right] (p_t/d_w)^{0.0686} \left[ 0.6759 Re_p^{-0.3897} \right]$$

Crown Copyright © 2012 Published by Elsevier Ltd. All rights reserved.

### Contents

1. Introduction . . . . .	6263
2. Aims and objectives . . . . .	6263
3. Experimental set-up . . . . .	6263

\* Corresponding author. Tel.: +91 755 266 0857.

E-mail addresses: [mukeshlalji@rediffmail.com](mailto:mukeshlalji@rediffmail.com),  
[Mukeshlalji10@yahoo.com](mailto:Mukeshlalji10@yahoo.com) (M.K. Lalji).

4. Experiential procedure.....	6265
5. Exergy $E$ .....	6266
5.1. Dimensionless exergy $E_D$ .....	6266
6. Validation of experimental set-up.....	6266
7. Results and discussion.....	6266
8. Conclusion.....	6266
References.....	6266

## 1. Introduction

Solar air heaters are generally used for low to moderate thermal energy requirements. These systems are cheap and easy to maintain, but due to the disadvantage of low thermal efficiency and because of low convective heat transfer coefficient between the absorber plate and the energy extracting carrier fluid, air. Several methods have been proposed for the enhancement of heat transfer coefficient of such collectors. Use of porous packing material in the collector duct is one of the methods. It considerably enhances the energy collection rate by increasing heat transfer rate between a carrier fluid and the absorber of the solar duct.

Various researchers have investigative use of passive technique for heat transfer enhancement in circular tubes, rectangular and square channels and correlation have been developed for duct with two opposite roughened heated walls. But solar air heater has only one wall as the heat transfer in surface that mix flow characteristics altogether different from that of two heated walls.

Literaturereview for fluid flow characteristics and heat transfer is done for various heat transfer enhancement techniques.

Packed bed solar air heater has been extensively investigated for low porosity system. However performance for high porosity and matrix shape is yet to be done.

A solar air heater is a simple device for heating air by utilizing solar energy. Various designs of solar air heater with different configuration have been proposed to enhance thermal performance of solar air heater by various investigators [1–15]. Gupta et al. [1] carried comparative study of various types of artificial roughness geometries in the absorber plate of solar air heater duct and their characteristics, investigated for the heat transfer, friction characteristics, energy and exergy analysis. Naphon [2] studied performance and entropy generation of the double-pass flat plate solar air heater with longitudinal fins. The effects of the inlet condition of working fluid and dimension of the solar air heater on the heat transfer characteristics, performance, and entropy generation were considered. Dhiman et al. [3] studied an analytical model describing the various temperatures and heat transfer characteristics of a parallel flow packed bed solar air heater PFPBSAH to study the effects of the mass flow rate and varying porosities of the packed material on its thermal performance. The friction in channels is dominant parameter in determining the effective thermal efficiency of the heater. Velmurugan and Ramesh [4] evaluated thermal performance of wire mesh solar air heater by employing a low carbon steel wire mesh a 5% increase in overall efficiency is observed when compared with conventional system. The present investigation is taken up with the objective of experimentation on wire screen matrix to collect data on heat transfer and fluid flow characteristics. The data is presented in the form of Nusselt number, friction factor and dimensionless exergy loss plot to bring out clearly the effect of parameters.

In short, it can be stated that by providing matrix shaped porosity material, considerable enhancement in thermal performance can be

achieved. Heat transfer and friction factor correlations developed in this work can be used for design of solar air heaters.

## 2. Aims and objectives

1. To study various methods for enhancement of efficiency of solar air heater using packed beds.
2. To study performance of packed bed solar air heater for high porosity range and for different shapes of matrices.
3. Design and development of experimental test setup of packed bed solar air heater as per ASHRAE (American Society for Heat transfer, Refrigeration & Air-conditioning Engineers) standards for the investigation of heat transfer coefficient and friction factor.
4. Performance evaluation of packed bed Solar air heater using wire mesh screen matrices of different shapes
5. Development of correlations for heat transfer coefficient and friction factor for packed bed solar air heater and its comparison with conventional design.
6. Exergy analysis of packed bed solar air heater.

## 3. Experimental set-up

The experimental set-up used in the present investigation, as shown in Fig. 1 was designed, fabricated, installed and used for date collection on heat transfer and fluid flow characteristics of solar air heaters with pocked bed and without pocked bed as per ASHRAE [13]. It consist of test section having two identical ducts, one smooth duct like that in a solar air heater in common use and the other one is similar but provided with a packed bed using wire screen matrices (Tables 1–3).

1. Both the duct had an identical length of 1.6 m width of 0.62 m and depth of 0.25 m. Having  $D_h=0.048$  and were made of softwood, both inclined at an angle of  $25^\circ$  to the horizontal.
2. The smooth or conventional duct fig had an absorber plate of 2 mm GI sheet. It was blackened with black board paint on the side facing solar radiation. It had a 3 mm thick glass sheet cover fixed 20 mm above the absorber plate. The side and bottom of the duct were insulated with thermocol sheet Thermocol is a commercial insulation of formed polystyrene having thermal conductivity 0.037 W/mK. The reason for using two duct in the present set puwas to compare the performance at the same operating condition such as mass flow rate, insolation and inlet fluid temperature.
3. The packed bet duct as shown in Fig. 1 had a 2 mm GI sheet having several layers of wire mesh screen arranged one above the other on the on the upper side of the GI sheet while below it there was a 50 mm of thermocol and 12 mm plywood. The sides were made of softwood 25 mm thick. A glass cover was provided on the upper side which rested on batons fitted adjacent to the side wall at a height of 25 mm. Another glass

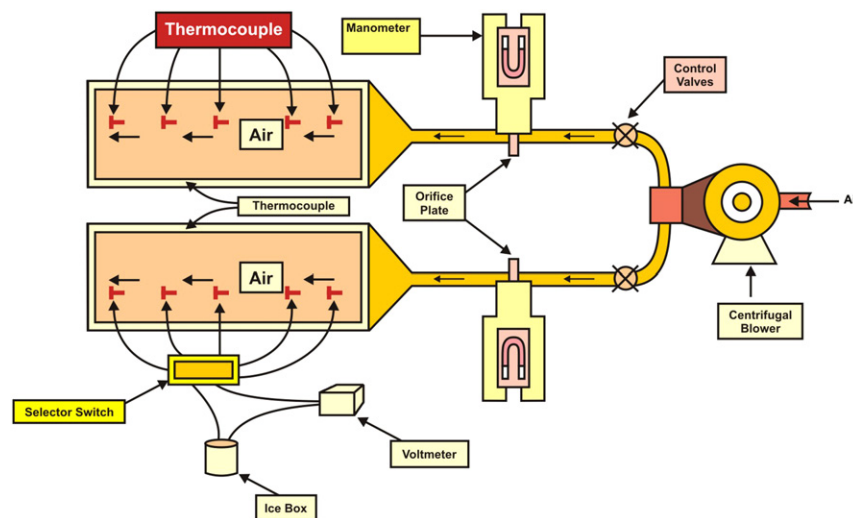


Fig. 1. Schematic diagram of experimental set-up.

**Table 1**  
Experimental data for porous absorber matrix S-3.

Run No.	$(\Delta h)_o$ , mm <sup>a</sup>	$(\Delta h)_d$ , mm, methyl alcohol	Inlet air temp. ( $T_i$ ), °C	Plate temperature (°C)									Bulk outlet air temp. ( $T_o$ )
				$T_1$	$T_2$	$T_3$	$T_4$	$T_5$	$T_6$	$T_7$	$T_8$	$T_9$	
1	77	3.0288	1.49	2.14	2.19	2.24	2.32	2.42	2.52	2.58	2.28	2.2	2.09
2	88	3.4038	1.49	2.12	2.17	2.22	2.30	2.38	2.48	2.54	2.24	2.16	2.06
3	100	3.7788	1.49	2.08	2.15	2.19	2.27	2.35	2.45	2.51	2.21	2.13	2.03
4	113	4.1827	1.49	2.06	2.14	2.17	2.25	2.32	2.42	2.46	2.16	2.09	2.00
5	128	4.5576	1.49	2.04	2.13	2.16	2.22	2.29	2.39	2.43	2.15	2.08	1.98
6	143	4.9615	1.49	2.01	2.11	2.13	2.18	2.25	2.35	2.40	2.13	2.06	1.95
7	158	5.4807	1.49	1.98	2.09	2.10	2.14	2.21	2.31	2.37	2.08	2.03	1.93

<sup>a</sup> Actual experimental data.

**Table 2**  
Experimental data for porous absorber matrix S-3.

Run no.	$(\Delta h)_o$ , mm <sup>a</sup>	$(\Delta h)_d$ , mm, methyl alcohol	Inlet air temp. ( $T_i$ )	Plate temperature (°C)									Bulk outlet air temp.
				$T_{11}$	$T_2$	$T_3$	$T_4$	$T_5$	$T_6$	$T_7$	$T_8$	$T_9$	
1	77	3.0288	42.0	57.79	59.03	60.26	62.23	64.69	67.15	68.63	61.24	59.27	56.8
2	88	3.4038	42.0	57.31	58.54	59.77	61.74	63.70	66.16	67.64	60.26	58.29	55.9
3	100	3.7788	42.0	56.32	58.05	59.03	60.99	62.96	65.43	66.90	59.52	57.55	55.2
4	113	4.1827	42.0	55.83	57.79	58.54	60.50	62.23	64.69	65.67	58.29	56.27	54.5
5	128	4.5576	42.0	55.34	57.55	58.29	59.77	61.49	63.95	64.94	58.05	56.32	53.9
6	143	4.9615	42.0	54.60	57.06	57.55	58.78	60.51	62.97	64.19	57.55	55.83	53.2
7	158	5.4807	42.0	53.86	56.57	56.81	57.79	59.52	61.98	63.46	56.32	55.09	52.5

<sup>a</sup> Actual experimental data.

**Table 3**  
Results for porous absorber matrix S-3.

S. no.	$T_i$ (°C)	$T_o$ (°C)	$T_p$ (°C)	$G_o$ (kg/s)	$f_r$	Re	$h$ (W/m <sup>2</sup> K)	$h_v$ (W/m <sup>2</sup> K)	$J_h$	Dimensionless
1	42.0	56.8	62.2	1.5581	0.0885	1959	6.93	1222	0.00348	16.73
2	42.0	55.9	61.4	1.6669	0.03028	2098	7.15	1262	0.00336	15.99
3	42.0	55.2	60.8	1.7779	0.0266	2239	7.39	1304	0.00325	15.32
4	42.0	54.5	60.1	1.8909	0.0235	2384	7.66	1352	0.00317	14.66
5	42.0	53.9	59.6	2.0135	0.0208	2540	7.90	1395	0.00307	14.07
6	42.0	53.2	58.8	2.01294	0.0186	2688	8.18	1444	0.00301	13.50
7	42.0	52.5	58.1	2.2394	0.0168	2829	8.37	1478	0.00293	13.06

cover was fixed at a height of 20 mm above the first one and supported on the frame, leaving a stagnant air gap of 20 mm between the two glass cover (Figs. 2 and 3).

4. A wooden exit section provided at the outlet of the test duct was followed by a mixing device, namely baffles for mixing the air. The exit section reduced the effect of sudden change

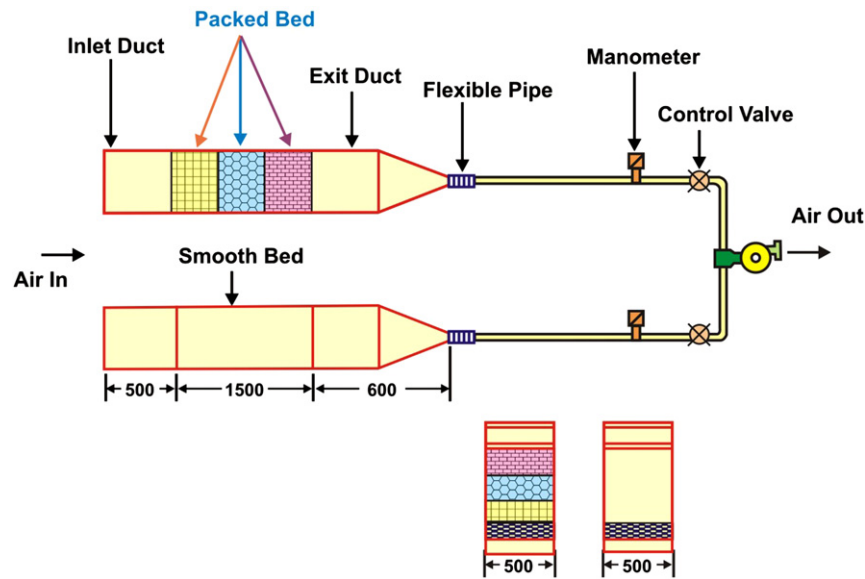


Fig. 2. Details of experimental set-up.

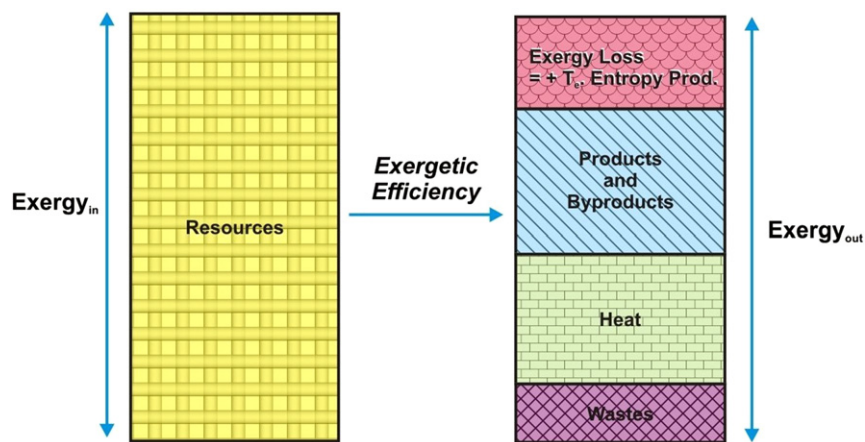


Fig. 3. Second law analysis of a real process of exergy.

on the rest section. The mixing device enabled measure of the bulk mean temperature at the outlet of the test section. The cross section area matched with that of the test duct. Three equally spaced baffle plates at the exit section were provided for the purpose of mixing the hot air coming out of the solar collector to obtain a uniform temperature of the air at outlet.

5. The mixing section was connected to the MILD STEEL pipe fitting through a transition piece and flexible pipes.
6. A 2.2 kW 3.0 h.p. centrifugal blower was used for drawing air through the duct.
7. Calibrated orifice plates, one in each were used to measure the air flow rates in both ducts. The orifice plate arrangement was designed for the flow measurement in the pipe. The orifice plate was fitted between the flanges, so align that it remained concentric with the pipe. The length of the pipe straight mild steel provided was based on pipe diameter  $d_1$ , which is minimum of  $10d_1$  on the upstream side and  $5d_1$  on the downstream side of the orifice plate.
8. Figure shows the dimensions of the packed bed, location of the pressure tap and layout of the thermocouple.

9. The temperature distribution in the bed of the test section was measured by means of pre-calibrated copper-constantan thermocouples and temperature of the air at the inlet and outlet were measured by digital thermometer.
10. Digital micro-voltmeter was used to indicate the output of the thermocouple in  $^{\circ}\text{C}$ , the temperature measurement system was calibrated to yield temperature values  $t \pm 0.1^{\circ}\text{C}$ .
11. The pressure drop across the test section was measured by using calibrated micro-manometers

#### 4. Experiential procedure

The experiment data was collected by following procedure described in ASHARE [13] for testing the solar air collector. Data pertaining to a given mass flow rate at an interval of 45 min were taken on a clear sky day. Before starting the experiment, all the joints of duct, inlet section, mixing device and pipe fitting were examined for leakage.

The blower was run for an hour and thereafter, the thermocouple readings for wire mesh temperatures at various locations and inlet and outlet air temperatures, pyranometer readings for intensity of solar radiation and manometer readings for pressure drop across the duct were recorded for a particular day. Experimental data were collected for flow rates ranging from 0.027–0.033 kg/s.

## 5. Exergy $E$

$$E = mC_p\Delta T - mC_p \ln T_o/T_i - RT_e \ln P_o/P_i + IA(1 - T_e/T_s).$$

### 5.1. Dimensionless exergy $E_D$

$$E_D = E/Q = T_e/\Delta T \ln T_o/T_i - P_o/P_i^{k-1/k} + \eta(1 - T_e/T_s).$$

## 6. Validation of experimental set-up

Before collecting the data from the experimental setup, the system was tested for validity by experimentation on a smooth duct to determine the Nusselt number and the friction factor. These values of the Nusselt number and the friction factor were compared with those obtained from the Dittus and Boelter correlation and Blasius equation given in S.K. Saini and R.P. Saini. The Nusselt number has a maximum deviation of 18% while the maximum deviation of the friction factor is 8.99% from the predicted values by the Dittus and Boelter.

The Nusselt number for a smooth rectangular duct is given by Dittus and Boelter is given below:

$$Nu_s = 0.024 Re^{0.8} Pr^{0.4}$$

The modified Blasius equation was as given below:

$$F_s = 0.085 Re^{-0.25}.$$

## 7. Results and discussion

The variation of Nusselt number with Reynolds number is shown in Fig. 4 and variation of friction factor with Reynolds number is given in Fig. 5.

Nusselt number increases as Reynolds number increase, also from the figure it is clear that as porosities reduces in the duct, Nusselt number increases as decrease in porosity increases turbulence and there by increases Nusselt number.

The above figure shows Dimensionless Exergy Loss for all matrices. From the two figures it is seen that S6 matrix has lowest dimensionless exergy loss and H3 matrix highest. S6 matrix has highest heat transfer enhancement which reduces the losses to the surroundings and H3 matrix has lowest heat transfer enhancement. This explains variation of the two curves.

## 8. Conclusion

On the basis of this investigation on heat transfer characteristics in packed bed solar air duct, it is concluded that the packed bed solar air heater having lower porosity performs better than higher porosity due to greater turbulence. Also exergy loss is less in case of lower porosity system due to higher heat transfer coefficient that leads to lesser losses to the atmosphere. Dimensionless exergy loss is more in case of matrix with high porosity.

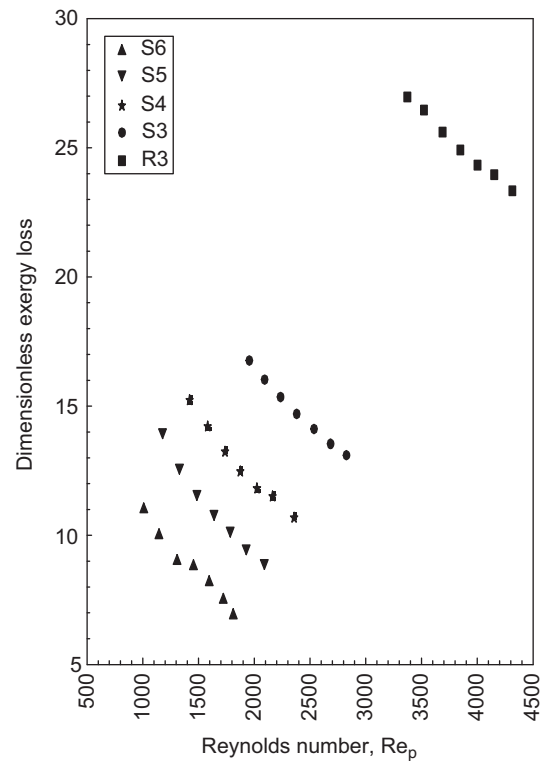


Fig. 4. Variation of dimensionless exergy loss for different matrices.

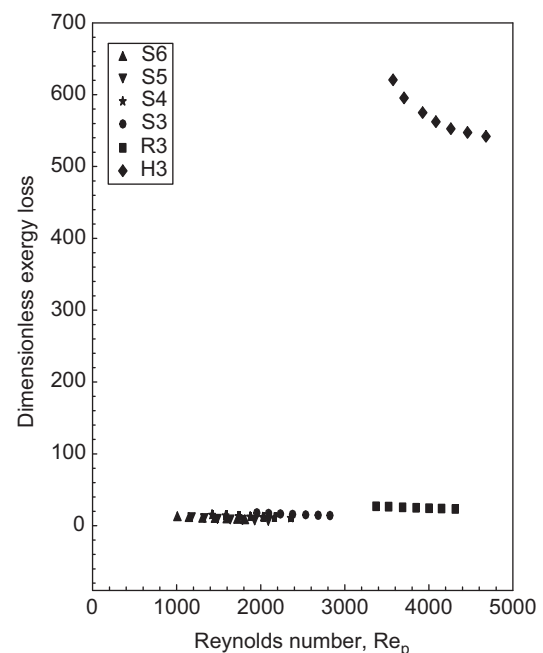


Fig. 5. Variation of dimensionless exergy loss for all matrices.

Maximum Dimensionless exergy loss occurs in lower Reynolds number region.

## References

- [1] Gupta MK, Kaushik SC. Performance evaluation of solar air heater having expanded metal mesh as artificial roughness on absorber plate. *Thermal Sciences* 2009;48:1007–16.

- [2] Naphon P. On the performance and entropy generation of the double-pass solar air heater with longitudinal fins. *Renewable Energy* 2006;30:1345–57.
- [3] Dhiman P, Thakur NS, Kumar A, Singh S. An analytical model to predict the thermal performance of a novel parallel flow packed bed solar air heater. *Applied Energy* 2011;88:2157–67.
- [4] Velmurugan P, Ramesh P. Evaluation of thermal performance of wire mesh solar air heater. *Indian Institute of Science & Technology* 2011;4(1):12–4.
- [5] Mittal MK, Varshney L. Optimal thermohydraulic performance of a wire mesh packed solar air heater. *Solar Energy* 2006;80:1112–20.
- [6] Varshney L, Saini JS. Heat transfer and friction factor correlations for rectangular solar air heater duct packed with wire screen matrices. *Solar Energy* 1998;62(4):255–62.
- [7] Singh R, Saini RP, Saini JS. Nusselt number and friction factor correlations for packed bed solar energy storage system having large sized elements of different shapes. *Solar Energy* 2006;80:760–71.
- [8] Thakur NS, Saini JS, Solanki SC. Heat transfer and friction factor correlations for packed bed solar air heater for a low porosity system. *Solar Energy* 2003;74:319–29.
- [9] Paswan MK, Sharma SP. Thermal performance of wire-mesh roughened solar air heaters. *ARISER* 2009;5(1):31–40.
- [10] Paul B, Saini JS. Optimization of bed parameters for packed bed solar energy collection system. *Renewable Energy* 2004;29:1863–76.
- [11] Choudhury C, Garg HP, Prakash J. Design studies of packed-bed solar air heaters. *Energy Conversion Management* 1993;34(2):125–38.
- [12] El-Sebaei AA, Aboul-Enein S, MRI Ramadan, Shalaby SM, Moharram BM. Thermal performance investigation of double pass-finned plate solar air heater. *Applied Energy* 2011;88:1727–39.
- [13] ASHRAE Standard 93-77. Method of testing to determine the thermal performance of solar air heater. New York; 1977. p. 1–34.
- [14] Shukla M, Pankaj BTambe. Predictive modelling of surface roughness and kerf widths in abrasive water jet cutting of Kevlar composites using neural network. *International Journal of Machining and Machinability of Materials* 2010;8(1–2):226–46.
- [15] Velmurugan P, Ramesh P. Evaluation of thermal performance of wire mesh solar air heater. *Indian Institute of Science & Technology* 2011;4(1):12–4.